Acta Crystallographica Section D
Biological Crystallography
ISSN 0907-4449

Membrane-protein crystallization *in cubo*: temperature-dependent phase behaviour of monoolein–detergent mixtures

Charles Sennoga,[a] Andrew Heron,[a] John M. Seddon,[a] Richard H. Templer[a] and Ben Hankamer[b]*

[a]Department of Chemistry, Imperial College of Science, Technology and Medicine, Exhibition Road, London SW7 2AY, England, and [b]Institute of Molecular Bioscience, University of Queensland, St Lucia Campus, Brisbane, Queensland 4072, Australia

Correspondence e-mail: b.hankamer@imb.uq.edu.au

Received 22 May 2002
Accepted 13 November 2002

The lipidic cubic phase of monoolein has proved to be a matrix well suited to the production of three-dimensional crystals of membrane proteins. It consists of a single continuous bilayer, which is contorted in three-dimensional space and separates two distinct water channels. It has previously been proposed that on the addition of precipitants, membrane proteins embedded in the cubic phase migrate through the matrix to nucleation sites and that this process is dependent upon the stability of the lipidic cubic phase. Here, the effect of detergent type (C_8–C_{12} glucosides, C_8–C_{12} maltosides and C_7 thioglucoside) and concentration (1–3× the critical micelle concentration; CMC) on cubic phase stability are reported in the form of the temperature-dependent phase behaviour (268–313 K) in 40% aqueous solution. The results are tabulated to show the best monoolein (MO)–detergent mixtures, mixing temperatures and crystallization temperatures identified. Monoolein–detergent mixtures suited for low-temperature *in cubo* crystallization of temperature-sensitive proteins are also reported for the first time. These mixtures can be prepared at low temperatures (mixed at $\leq$288 K) and remain stable at 277 K for a period of at least one month. They include MO–heptyl thioglucoside (1× and 3× CMC), MO–nonyl glucoside (3× CMC), MO–octyl maltoside (3× CMC), MO–nonyl maltoside (1× CMC) and MO–decyl maltoside (1× CMC).

1. Introduction

One of the great challenges of cell biology is solving the atomic structures of membrane proteins. Recently, cubic phase, or *in cubo*, crystallization has yielded five well ordered three-dimensional crystals of membrane proteins, including those of bacteriorhodopsin, halorhodopsin, sensory rhodopsin and the reaction centres of the purple bacteria *Rhodobacter sphaeroides* and *Rhodopseudomonas viridis* (Luecke *et al.*, 1999; Chiu *et al.*, 2000; Kolbe *et al.*, 2000; Royant *et al.*, 2001). As its name suggests, the method relies upon the use of lipids such as monoolein (MO) that are able to form bicontinuous cubic phases. Lipidic bicontinuous cubic phases are complex three-dimensional lipid networks consisting of a single continuous bilayer intricately arranged within three-dimensional space and bounded by two distinct water channels (Templer, 1998). The most common of these are the *Im*3*m*, *Ia*3*d* and *Pn*3*m* phases, which are mathematically related. Despite the success in obtaining well ordered crystals, the mechanisms underlying crystal production *in cubo* are a matter of considerable debate. Cubic phase crystallization is most commonly portrayed as a hybrid between two- and three-dimensional crystallogenesis, with the crystallization process divided into two theoretical stages: the protein insertion (Figs. 1*a* and 1*b*) and crystallization (Figs. 1*c* and 1*d*)

stages (Caffrey, 2000; (Nollert *et al.*, 2002). The first is proposed to involve a lamellar-to-cubic phase transition, while the reverse transition occurs during the crystallization stage of the process.

During the insertion process (Fig. 1*a*), the aqueous detergent–protein solution is mixed with dry monoolein (MO) or other cubic phase lipids of choice (Landau & Rosenbusch, 1996; Cheng *et al.*, 1998; Rummel *et al.*, 1998). As water diffuses into the lipid (Fig. 1*a*), the protein and detergent concentrations in the aqueous phase are proposed to increase, inducing the formation of a detergent-rich lamellar phase in which the membrane proteins are embedded (Nollert *et al.*, 2001). Upon complete hydration of the MO, an equilibrium is reached in which all of the lipid is thought to relax into a uniform bicontinuous cubic phase containing the embedded membrane proteins (Fig. 1*b*). It is proposed that the membrane proteins insert into the bilayer network separating these water channels (ringed in red and green in Fig. 1*b*) and can subsequently diffuse freely through its three-dimensional volume (Caffrey, 2000; Nollert *et al.*, 2001). The cubic phase lipid bilayer can thus be considered to be a three-dimensional network facilitating protein diffusion to and from nucleation sites and crystals.

To induce crystallization, solid salts, concentrated salt solutions or buffered PEG stocks are usually added (Fig. 1*c*). These dehydrate the cubic phase and may provide counterions to favour protein–protein contacts during crystal formation (Nollert *et al.*, 2001). It is reported that during dehydration the curvature of the bilayer towards the water rises, resulting in two major changes (Seddon *et al.*, 1997; Templer, 1998). Firstly, it becomes energetically favourable for the lipid cubic phase to undergo localized cubic-to-lamellar phase transitions (Figs. 1*c* and 1*d*). Secondly, the increased curvature of the cubic phase makes it energetically favourable for the proteins to enter the lamellar phase (Fig. 1*d*). Indeed, when crystallized *in cubo*, bacteriorhodopsin (Luecke *et al.*, 2000; Pebay-Peyroula *et al.*, 2000), halorhodopsin (Luecke *et al.*, 1999) and sensory rhodopsin (Royant *et al.*, 2001) molecules were all found to be arranged in stacked lamellar arrays within the crystal. The high order of these crystals is reflected in the high-resolution structures that they yield (1.55–2.1 Å) and provides further evidence for a cubic-to-lamellar transformation at a localized level.

The crystallization process summarized in Fig. 1 is a useful model of the experimental purposes which now requires testing and refining if the full potential of the *in cubo* process is to be achieved. The focus of this paper is the role played by lipid-phase inter-conversion: lamellar-to-cubic (Figs. 1*a* and 1*b*) during protein insertion and cubic-to-lamellar (Figs. 1*c* and 1*d*) during crystallization (Caffrey, 2000; Nollert *et al.*, 2001). Here, we report the effect of temperature, detergent type and concentration on these interconversion processes and use the information gained to propose new *in cubo* crystallization strategies for membrane proteins, including low-temperature protocols for temperature-sensitive proteins.

2. Methods

2.1. Preparation of monoloein–detergent mixtures

Monoolein (MO; >99.9%; Larodan Fine Chemicals, Sweden), C_7–C_{12} alkyl glucoside homologues of β-D-malto-

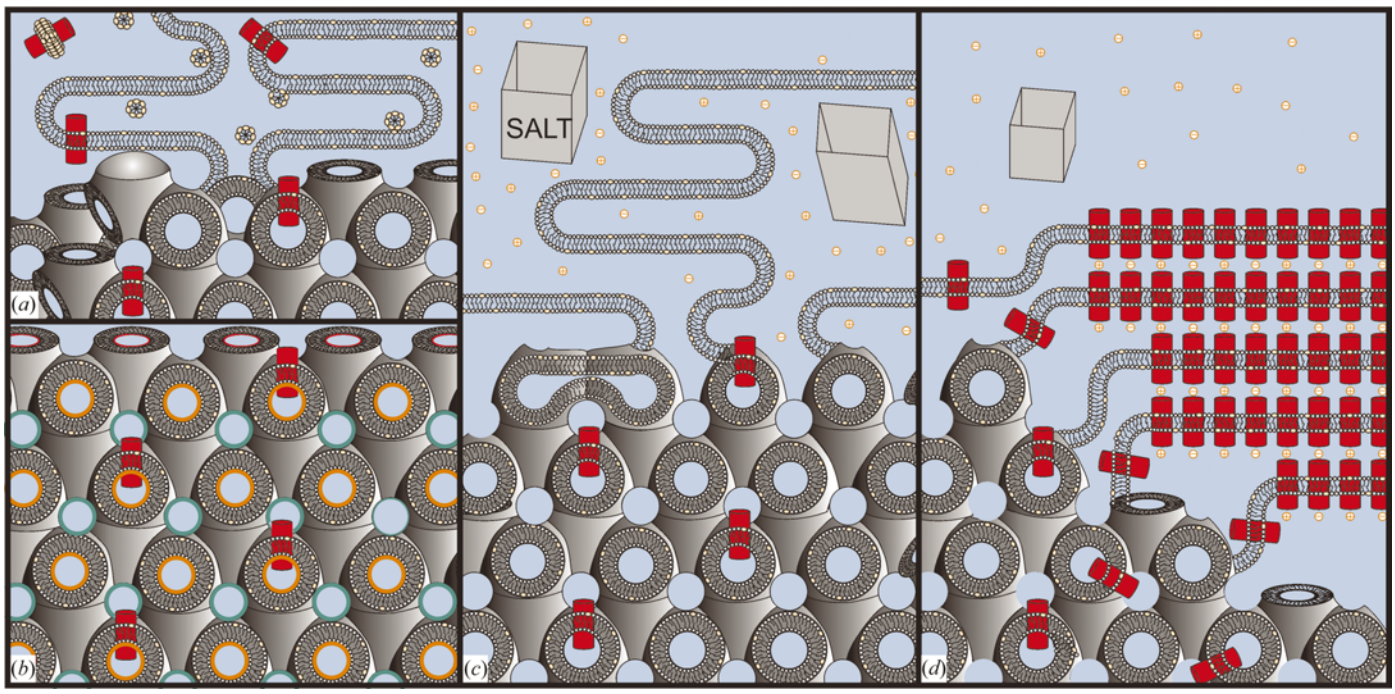

Figure 1
The proposed cubic phase crystallization process. The process can be divided into four stages: (*a*) protein insertion, (*b*) equilibrium of the protein-loaded cubic phase, (*c*) salt-induced dehydration of the cubic phase matrix and (*d*) nucleation and crystal growth (see text for details). This figure is based on the work of Landau & Rosenbusch (1996), Nollert *et al.* (2001) and the review by Caffrey (2000).

Table 1
Critical micelle concentrations of the detergents tested.

Detergent	CMC (m*M*)
Octyl glucoside (OG)	19.0
Nonyl glucoside (NG)	6.5
Decyl glucoside (DG)	2.2
Dodecyl glucoside (DDG)	0.19
Octyl maltoside (OM)	19.5
Nonyl maltoside (NM)	6.0
Decyl maltoside (DM)	1.8
Unadecyl maltoside (UM)	0.59
Dodecyl maltoside (DDM)	0.18
Heptyl thioglucoside (HTG)	29.0

sides and β-D-glucosides, together with heptyl-β-D-thioglucoside (Anatrace, USA) detergents were used without further purification. Detergent stocks of one to three times the critical micelle concentration (CMC) were prepared in HPLC-grade water (BDH Chemicals) (see Table 1). These concentrations were selected as they encompass the most commonly used concentrations employed to produce monodisperse solutions of membrane proteins for three-dimensional crystallization. MO–detergent mixtures were prepared by combining the components in a ratio of 60:40(*w*:*v*) MO:detergent stock solution. The mixture was then subjected to six freeze–thaw cycles (258–313 K) and inspected under a polarizing-light microscope to ensure the formation of a homogeneous microstructure. Under polarizing light, cubic phases appear dark, being optically isotropic and non-birefringent. In contrast, lamellar phases appear bright with a defined microstructure covered with Maltese crosses of light. The homogeneous samples were transferred to X-ray transparent capillaries having a diameter of 1.5 mm (W. Müller, Germany), which were then flame-sealed and incubated overnight before cooling to 258 K for 1 h prior to X-ray data collection.

2.2. X-ray measurements

2.2.1. Determining the phase behaviour of MO–detergent mixtures. Time-resolved X-ray diffraction measurements were made over the temperature range 258–313 K to determine the phases and unit-cell parameters of all 60:40(*w*:*v*) MO:detergent mixtures. The X-ray diffractometer used was specially constructed. Partial monochromatization was achieved with a nickel filter selecting the Cu $K\alpha$ lines (λ = 1.542 Å) sampled at shallow angles from a GX-20 rotating-anode generator (Enraf–Nonius, Netherlands) using a 100 µm focus cup with a loading of 750 W. X-ray focusing was achieved using Franks quartz double-mirror optics in a cross-coupled arrangement with a 200 mm focal length, thus delivering a beam spot 160 × 110 µm at full-width at half-maximum (FWHM). During X-ray measurements, a set of adjustable tungsten slits approximately 15 mm before the sample reduced parasitic scattering to levels where we were able to measure lattice spacings up to 300 Å. Sample capillaries were placed in a copper sample holder with thermoelectric temperature control between 258 and 318 K. Temperature control was measured to be within ±0.03 K. The optics and the sample cell were both held under vacuum to minimize air scatter. The sample chamber included a variable-length evacuated flight path, allowing the X-ray detector to be placed between 120 and 300 mm from the sample, thereby taking advantage of the long focal depth of the optics. The design was limited to wide-angle measurements down to a minimum spacing of 3.5 Å. The time-resolved diffracted intensity was recorded on an image-intensified CCD-based two-dimensional detector. The entire X-ray system was computer controlled, allowing automated data acquisition and analysis. The acquired powder-diffraction images were radially integrated and subsequently fitted using a parsed program environment, *TV*4 (created by E. F. Eikenberry and S. M. Gruner). All samples were allowed to equilibrate for at least 120 min after each 5 K temperature step before acquiring subsequent X-ray patterns. Repeated runs on a single sample using this protocol gave results which were reproducible to ±1.0 Å in the lattice parameter. Phase-transition temperatures measured on a single sample using this protocol were reproduced to ±1 K.

2.2.2. Assessing 277 K stability. A low-temperature crystallization strategy (277 K) has the potential to improve the

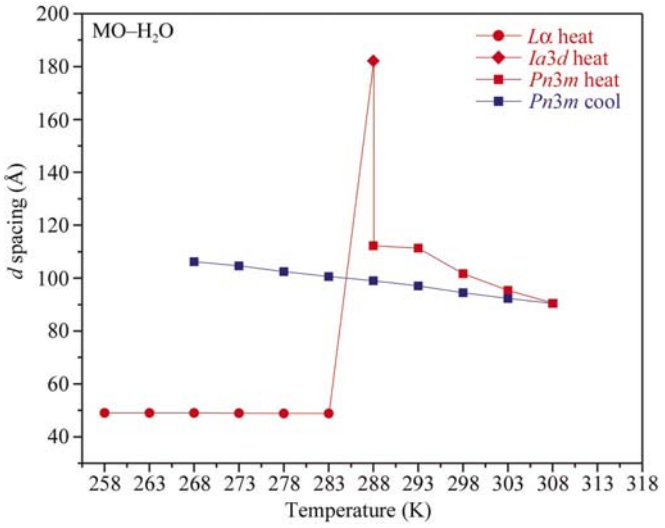

Figure 2
Temperature-dependent phase behaviour of a 60:40(*w*:*v*) MO:H_2O mixture. The MO–H_2O mixture was prepared at 293 K and subjected to six freeze–thaw cycles (258–313 K). It was then inspected under a polarizing-light microscope to ensure the formation of a homogeneous cubic phase. The sample was then heated (red data set) to 308 K. Upon reaching the maximum temperature, the sample was cooled (blue data set) to 268 K. The phase type at a given temperature is indicated by the denoted symbols. Heating the sample from 258 K (red) induces a marked transition from the $L\alpha$ to the *Ia*3*d* phase between 283 and 288 K. Further heating induces a rapid transition from the *Ia*3*d* to the *Pn*3*m* phase (288 K). Temperature increases between 288 and 308 K do not induce a further phase transition, but slight changes in the *Pn*3*m* lattice parameters are observed. Cooling the sample from 308 K (blue) results in a markedly different phase behaviour to that observed on heating, in that the sample remained in the *Pn*3*m* phase all the way down to 268 K. The only change observed on cooling is an increase in the *Pn*3*m* lattice parameter, which was of the order of 15%. This control clearly illustrates the metastability of this phase at 60:40(*w*:*v*) MO:H_2O composition.

crystal quality of temperature-sensitive proteins. To facilitate the development of a systematic low-temperature crystallization screen, the metastability of the cubic phase was investigated upon cooling from 313 to 277 K. The sample temperature was then held at 277 K for one month prior to taking X-ray diffraction measurements.

3. Results and discussion

3.1. Temperature-dependent phase transitions of a water–MO mixture

A prerequisite for *in cubo* crystallization in monoolein is the identification of conditions that support the existence of a stable 'bulk' cubic phase, given that the process occurs within its gel-like matrix. The phase behaviour of monoolein is directly dependent on its metastability (Fig. 2). When the monoolein–water mixture is heated from 273 to 313 K, it is supplied with the activation energy required to drive the *Lα*–*Ia3d*–*Pn3m* cubic phase transition *via* membrane-fusion events. To convert the *Pn3m* phase back to the *Lα* phase would require an even higher net energy input, as this process involves extensive scission of the bicontinuous cubic channels. However, this energy input is not provided when the *Pn3m* phase is cooled from 313 to 268 K (Fig. 2) and so, instead of converting back to *Lα*, it remains in the *Pn3m* phase, but in a metastable supercooled state. From this state, conversion back to the *Lα* phase takes a considerable time. Consequently, whereas the *Lα*–*Pn3m* cubic phase transition is observed on heating, the reverse is not observed on cooling.

3.2. Temperature-dependent phase transitions of detergent–MO mixtures

Pure monodisperse membrane proteins are generally required for the production of high-quality three-dimensional crystals (Luecke *et al.*, 1999; Chiu *et al.*, 2000; Kolbe *et al.*, 2000; Royant *et al.*, 2001), although it has been reported that bacteriorhodopsin can be crystallized *in cubo* directly from purple membranes (Nollert *et al.*, 1999). The addition of detergents to the monoolein–water mixture profoundly alters the phase behaviour observed in Fig. 2. To develop efficient large-scale cubic phase crystallization screens, it is therefore critical to

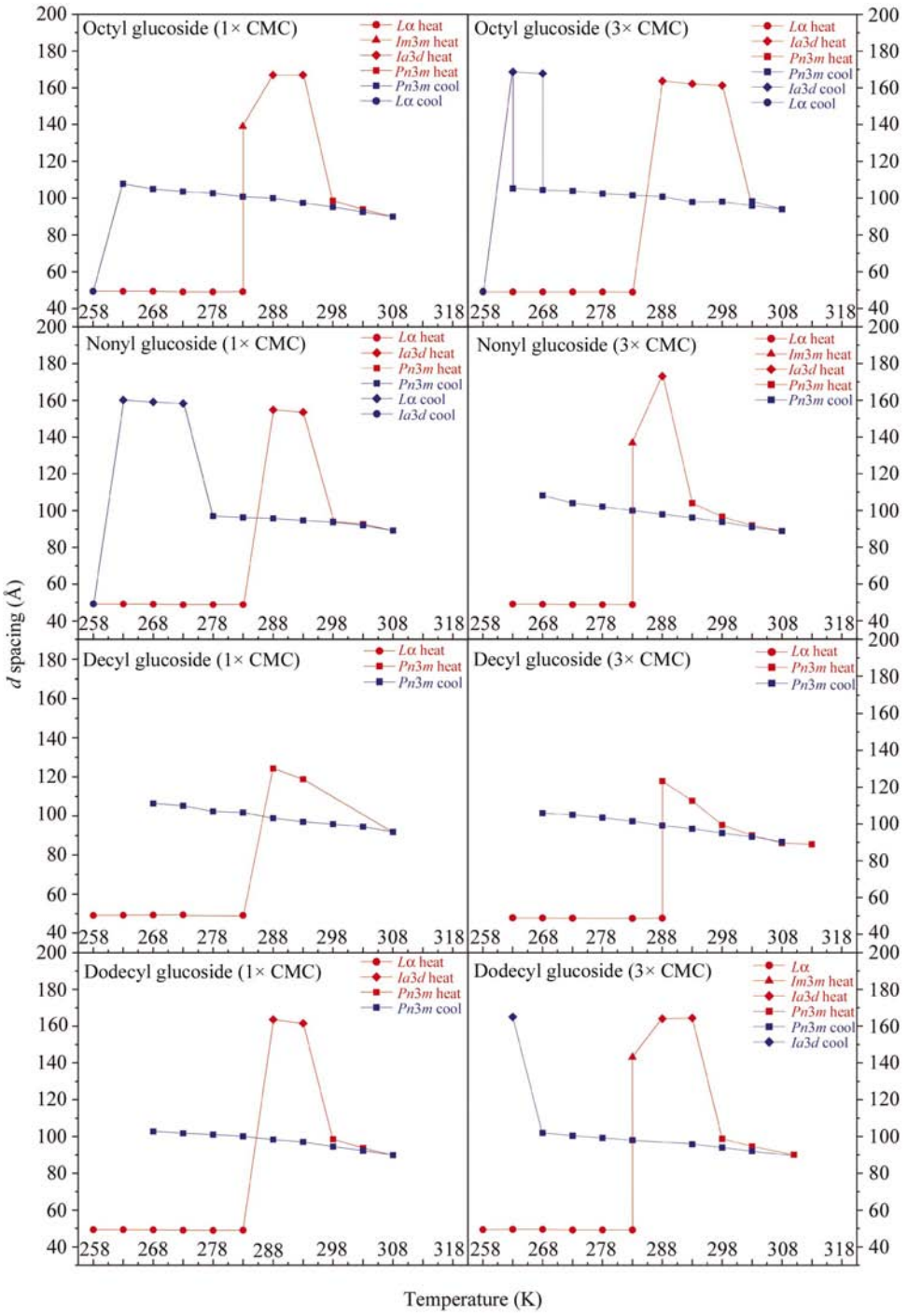

Figure 3
Temperature-dependent phase behaviour of 60:40(*w*:*v*) MO:glucoside mixtures. The left-hand and right-hand columns show the phase transitions determined for glucosides at 1× and 3× the CMC, respectively, in which their chain lengths increase from the top (C_8) to the bottom (C_{12}). The red and blue parts of each data set indicate the phase changes induced by sample heating and cooling, respectively. The phase type at a given temperature is indicated by the use of specific symbols, which are individually annotated for each MO–detergent mixture.

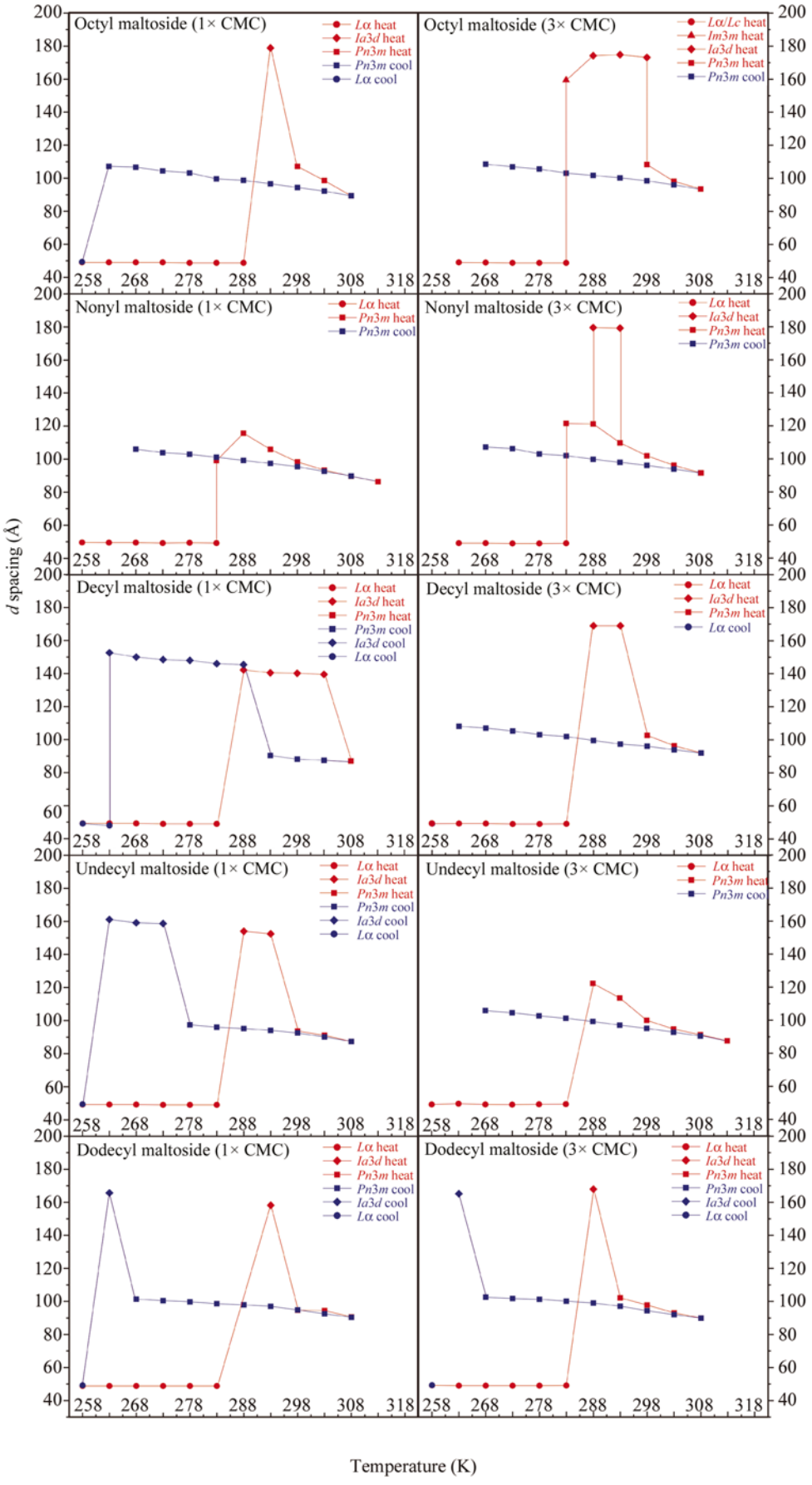

identify detergents that have the dual properties of solubilizing membrane proteins effectively, without causing detrimental effects on the cubic phase matrix, during the protein insertion step. For this purpose, the detailed temperature-dependent phase behaviour was determined for glucoside–MO (Fig. 3), maltoside–MO (Fig. 4) and heptyl thioglucoside–MO (Fig. 5) mixtures using detergent concentrations of one and three times the CMC and 60% MO. These detergents and concentration ranges were selected as they typically yield monodisperse proteins suitable for crystallization.

All of the glucoside, maltoside and thioglucoside mixtures analysed underwent a sharp *Lα*–cubic phase transition at 283–288 K upon heating (Figs. 3, 4 and 5). In many cases, the transition was directly from the *Lα* to the *Pn3m* phase. In the remaining cases, heating induces either an *Lα*–*Ia3d*–*Pn3m* or an *Lα*–*Im3m*–*Ia3d*–*Pn3m* transition. The *Lα*–*Ia3d*–*Pn3m* transition is consistent with the published MO–H_2O equilibrium phase diagram (Hyde *et al.*, 1984; Qiu & Caffrey, 2000). The *Lα*–*Im3m*–*Ia3d*–*Pn3m* transition observed for 1× octyl glucoside (OG), 3× dodecyl maltoside (DDG), 3× octyl maltoside (OM) and 3× nonyl glucoside (NG) has not been reported previously. Subsequent heating to 298 K yielded a pure

Figure 4
Temperature-dependent phase behaviour of 60:40(*w*:*v*) MO:maltoside mixtures. The left-hand and right-hand columns show the phase transitions determined for maltosides at 1× and 3× the CMC, respectively, in which their chain lengths increase from the top (C_8) to the bottom (C_{12}). The red and blue parts of each data set indicate the phase changes induced by sample heating and cooling, respectively. The phase type at a given temperature is indicated by the use of specific symbols, which are individually annotated for each MO–detergent mixture.

Pn3m phase in almost all cases (Figs. 3, 4 and 5). Once formed, the *Pn3m* phase remained stable both on heating (to 308–313 K) and in most cases on cooling to temperatures of 273 K. The latter is indicative of the metastability of the system and opens up the possibility of low-temperature *in cubo* crystallization of labile membrane proteins. Exceptions to the observed stability on cooling were 1× NG, 1× decyl maltoside (DM), 1× undecyl maltoside (UM) and 3× heptyl thioglucoside (HTG) samples, all of which formed the *Ia3d* or coexisting *Pn3m*–*Ia3d* phases rather than a pure *Pn3m* phase at low temperatures. In the case of glucoside and maltoside detergents, the same coexisting phase mixtures were not observed in the corresponding 3× CMC samples, possibly because the increase in surfactant concentration resulted in a reduction in the magnitude of the spontaneous curvature (H_0), thereby favouring phases with lower interfacial curvature such as *Pn3m* (rather than *Ia3d*) (Templer, 1998).

3.3. Implications for the protein-insertion step

The temperature-dependent phase behaviour shown in Figs. 3, 4 and 5 provides a detailed guide for production of specific cubic phases (*Im3m*, *Ia3d* and *Pn3m*) from dry monoolein using either the centrifugal (Landau & Rosenbusch, 1996) or syringe-mixing (Cheng *et al.*, 1998) method. Three specific pieces of information relating to the protein-insertion step can be gained. Firstly, all of the detergent–monolein mixtures tested underwent a sharp lamellar-to-cubic phase transition in the 283–293 K range. This indicates that to insert protein molecules directly into the *Im3m*, *Ia3d* or *Pn3m* cubic phases, mixing temperatures must be kept above the specific *Lα*–cubic transition temperature of a given detergent–MO mix. Secondly, by choosing a specific mixing temperature and MO–detergent blend, the type of cubic phase (*i.e. Im3m*, *Ia3d* or *Pn3m*) into which the protein is to be inserted can be defined. For example, the MO–decyl glucoside (1× CMC) mixture prepared at 288 K would be expected to yield a pure *Pn3m* cubic phase. Thirdly, as reduced mixing temperatures may be beneficial for temperature-sensitive proteins, specific MO–detergent mixtures capable of forming the desired cubic phase at reduced temperatures can be selected. In particular, Figs. 3, 4 and 5 show that pure *Pn3m* phases can be formed at temperatures as low as 272 K (1× DG, 3× DG and 3× UM) and below (1× HTG, 1× NM at ∼283 K). In a second though untested scenario, the temperature could be kept low to insert the protein into the *Lα* phase before inducing a lamellar-to-cubic phase transition through a short heating step. In the context of stabilizing temperature-sensitive membrane proteins, it is also worth noting that heat-induced damage may be reduced by using the syringe-mixing (2–5 min) rather than the centrifugal (1–2 h) mixing approach, as rapid insertion of the protein into the monoolein bilayer may in itself afford protection through the inward pressure exerted by the lipids on its membrane-spanning domains (Cantor, 1999).

3.4. Implications for the protein crystallization step

3.4.1. Low-temperature stability. To date, almost all cubic phase crystallization trials have been conducted at room temperature using relatively stable proteins (Chiu *et al.*, 2000). Such conditions are less likely to be suited for the crystallization of the large number of temperature-sensitive proteins available to crystallographers.

The metastability of the cubic phase matrix (Figs 2, 3, 4 and 5) suggests that once formed, the three-dimensional bilayer networks of monoolein–detergent mixtures are likely to be relatively robust both under constant-temperature conditions and upon cooling (Figs 3, 4 and 5; Table 2). To test this rigorously and to assess the stability of specific MO–detergent mixtures over long periods of time, all samples were incubated at 277 K for one month (Table 2). Given that the *in cubo* crystallization process generally occurs over a number of weeks, matrix stability over a one-month time frame is a prerequisite. The 1× CMC maltoside–MO cubic phases appeared to be most stable under these conditions. Raising the concentration of the maltoside detergent from 1× to 3× CMC reduced the stability of the cubic phase, as did the exchange of maltosides for glucosides (1× or 3× CMC), although they were preserved in the presence of the shorter chain glucosides (1× OG, 3× OG and 3× NG). Cubic phases also remained stable in the presence of 1× HTG and 3× HTG. To aid crystallographers, Table 2 provides a summary of the mixing and stability properties of the MO–detergent mixtures.

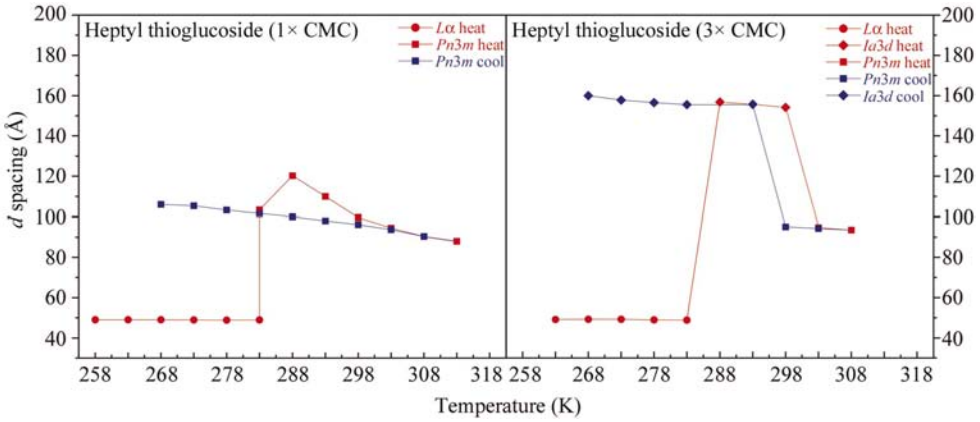

Figure 5
Temperature-dependent phase diagrams of 60:40(*w*:*v*) MO:heptyl thioglucoside mixtures. The left-hand and right-hand panels show the phase transitions determined for heptyl thioglucoside at 1× and 3× the CMC, respectively. The red and blue parts of the data set indicate phase changes induced by sample heating and cooling, respectively. The phase type at a given temperature is indicated by the use of specific symbols, which are individually annotated for the two MO–detergent mixtures.

3.4.2. Nucleation and crystal growth. The results presented allow the crystallographer to select conditions to prepare a specific cubic phase matrix. However, which of the cubic phases is best for the purpose of

Table 2
One-month stabilty test of MO–detergent mixtures at 277 K.

MO–detergent mixtures were incubated for one month at 277 K prior to the determination of their phases and lattice parameters. The lowest mixing temperatures that can be used to produce the observed cubic phases, based on Figs. 3, 4 and 5, are provided. For example, the MO–HTG (1× CMC) mixture yielded an *Pn3m* phase after one month of incubation at 277 K. Fig. 5 shows that the lowest mixing temperature capable of yielding the *Pn3m* phase from this mixture is 288 K.

	1× CMC			3× CMC		
	Phase (1 month)	Lattice parameters (Å)	Lowest mixing temp. (K)	Phase (1 month)	Lattice parameters (Å)	Lowest mixing temp. (K)
HTG	*Pn3m*	114.6	283	*Ia3d*	182.5	288
OG	*Pn3m*	101.7	298	*Pn3m*	103.1	303
NG	*Lα*	(49.0)	—	*Ia3d*	166.0	288
DG	*Lα*	(49.0)	—	*Lα*	(49.0)	—
DDG	*Lα*	(49.0)	—	*Lα*	(49.0)	—
OM	*Pn3m*	129.3	298	*Ia3d*	199.4	288
NM	*Pn3m*/*Ia3d*	116.0/187.0	283	*Lα*	(48.7)	—
DM	*Ia3d*	155.9	288	*Lα*	(49.1)	—
UM	*Pn3m*	98.5	298	*Lα*	(49)	—
DDM	*Pn3m*	98.1	298	*Pn3m*	115.2	293

high-quality crystal production is less clear. To aid the crystallographer in the choice of matrix, a number of similarilities and differences between the properties of the *Im3m*, *Ia3d* and *Pn3m* phases are highlighted.

The *Im3m*, *Ia3d* and *Pn3m* cubic phases have several similarities. Firstly, all three have mathematically related three-dimensional structures. This has important implications for the constraints on nucleation and crystal packing. Consider two protein molecules (*A* and *B*) with the same orientation perpendicular to the membrane plane, migrating from location 1 in a given three-dimensional cubic phase matrix to a second location, 2. No matter how convoluted the migration path of proteins *A* and *B* through the bulk *Im3m*, *Ia3d* or the *Pn3m* cubic phases, their orientation with respect to one another when they arrive at location 2 cannot be reversed unless defects exist in the lattice. Secondly, the fluidity of the bilayers is likely to be similar, suggesting that this factor is unlikely to alter the rate of protein diffusion to and from a nucleation site. Based on these similarities, it might be expected that the *Im3m*, *Ia3d* or the *Pn3m* phases are equally capable of supporting *in cubo* crystallization. However, there are a number of important differences between the systems that must be taken into account.

The first difference that should be taken into consideration is unit-cell size. The freedom of protein migration through the cubic phase matrix is dependent on the unit-cell size of the selected matrix. For example, a large membrane protein inserted into a cubic phase matrix with a small unit-cell size is likely to be restricted in its ability to migrate. The MO–water phase diagram (Caffrey, 2000) shows that the *Pn3m* phase is more hydrated than the *Ia3d* and so has the largest aqueous pores. The *Pn3m* phase would therefore be expected to provide the greater freedom of the movement for the hydrophilic domains of the embedded proteins. Secondly, as a direct consequence of the large pore size, the mean curvature of the bilayers in the *Pn3m* cubic phase is lower than that observed in the corresponding *Ia3d* phase. The addition of precipitants to a cubic phase matrix containing protein is thought to induce its dehydration and a concomitant increase in bilayer curvature (Cherezov *et al.*, 2001). As the *Pn3m* phase can undergo a higher degree of curvature change than the *Ia3d* cubic phase before converting to the lamellar phase, it is possible that a greater degree of hydrophobic mismatch between the bilayer and the hydrophobic domains of the protein is induced. This in turn might be expected to induce phase separation of the protein and subsequent nucleation (Israelachvili *et al.*, 1977).

4. Conclusion

The results presented show for the first time the detailed temperature-dependent phase behaviour of a wide range of 60% MO–detergent mixtures suited for membrane-protein crystallization. The results provide a framework for the development of more systematic cubic phase crystallization screens. In particular, the results presented can aid crystallographers in the production of *Im3m*, *Ia3d* and *Pn3m* cubic phase matrices and extend the method into the low-temperature range more suited to the crystallization of temperature-sensitive proteins.

The cubic phase crystallization approach itself has a number of potential advantages for the crystallization of membrane proteins. Firstly, it is already a proven technology, having yielded five well ordered membrane proteins including bacteriorhodopsin (diffracting to 1.55 Å; Luecke *et al.*, 1999), halorhodopsin (1.8 Å; Kolbe *et al.*, 2000), sensory rhodopsin (2.1 Å; Royant *et al.*, 2001), the reaction centre of *Rhodopseudomonas viridis* (3.7 Å; Chiu *et al.*, 2000) and the reaction centre of *Rhodobacter sphaeroides* (6 Å; Chiu *et al.*, 2000). Two of these crystals have yielded structures that are among the highest resolution of any membrane protein produced by any method. The method also facilitates the insertion of membrane proteins into a lipid bilayer within minutes (Cheng *et al.*, 1998) and so has the potential to stabilize labile membrane proteins rapidly through the lateral pressure exerted on their membrane-spanning domains by the bilayer (see Cantor, 1999). The *in cubo* approach also appears to favour the formation of type I over type II crystals (Luecke *et al.*, 1999; Kolbe *et al.*, 2000; Royant *et al.*, 2001). Proteins arrayed in type I crystals are generally more tightly packed owing to lower water content and reduced detergent-induced steric hindrance and so may be able to yield more highly diffracting crystals. Type I crystal packing also facilitates the crystallization of hydrophobic membrane proteins that are prevented from forming type II arrays by detergent-induced steric hindrance. A further advantage is that cubic phase crystals are lipid-based rather than detergent-based and therefore, in contrast to detergent-based three-dimensional crystals, are resistant to solubilization in aqueous solutions. This theoretically makes them less susceptible to damage induced by soaking with heavy-metal derivatives. Finally, monoolein can be used as a cryoprotectant in the protection of three-dimensional crystals against X-ray induced beam damage. Whereas detergent-based crystals have to be trans-

ferred to cryoprotectant solutions that often reduce crystal quality, crystals produced *in cubo* can be released from the cubic phase by lipase-catalysed digestion of the MO with the digestion products acting as a cryoprotectants (Nollert & Landau, 1998).

The authors would like to extend their thanks to the EPSRC, BBSRC and Unilever Research for financial support. We also acknowledge with gratitude the many helpful discussions with Jeff Abramson, Peter Nollert, Ehud Landau and Jim Barber and the critical reading of the manuscript (Peter Nollert and Jeff Abramson). The authors would also like to thank Karim Maghlaoui and Ulrike Wedemeyer for their excellent technical assistance.

References

Caffrey, M. (2000). *Curr. Opin. Struct. Biol.* **10**, 486–497.
Cantor, R. S. (1999). *Biophys. J.* **76**, 2625–2639.
Cheng, A., Hummel, B., Qiu, H. & Caffrey, M. (1998). *Chem. Phys. Lipids*, **95**, 11–21.
Cherezov, V., Fersi, H. & Caffrey, M. (2001). *Biophys. J.* **81**, 225–242.
Chiu, M. L., Nollert, P., Loewen, M. C., Belrhali, H., Pebay-Peyroula, E., Rosenbusch, J. P. & Landau, E. M. (2000). *Acta Cryst.* D**56**, 781–784.
Hyde, S., Andersson, B., Ericsson, B. & Larsson, K. (1984). *Z. Kristallogr.* **168**, 213–219.
Israelachvili, J. N., Mitchell, D. J. & Ninham, B. W. (1977). *Biochim. Biophys. Acta*, **470**, 185–201.
Kolbe, M., Besir, H., Essen, L. O. & Oesterhelt, D. (2000). *Science*, **288**, 1390–1396.
Landau, E. M. & Rosenbusch, J. P. (1996). *Proc. Natl Acad. Sci. USA*, **93**, 14532–14535.
Luecke, H., Schobert, B., Cartailler, J. P., Richter, H. T., Rosengarth, A., Needleman, R. & Lanyi, J. K. (2000). *J. Mol. Biol.* **300**, 1237–1255.
Luecke, H., Schobert, B., Richter, H. T., Cartailler, J. P. & Lanyi, J. K. (1999). *J. Mol. Biol.* **291**, 899–911.
Nollert, P. & Landau, E. M. (1998). *Biochem. Soc. Trans.* **26**, 709–713.
Nollert, P., Navarro, J. & Landau, E. M. (2002). *Methods Enzymol.* **343**, 183–199.
Nollert, P., Qiu, H., Caffrey, M., Rosenbusch, J. P. & Landau, E. M. (2001). *FEBS Lett.* **504**, 179–186.
Nollert, P., Royant, A., Pebay-Peyroula, E. & Landau, E. M. (1999). *FEBS Lett.* **457**, 205–208.
Pebay-Peyroula, E., Neutze, R. & Landau, E. M. (2000). *Biochim. Biophys. Acta*, **1460**, 119–132.
Qiu, H. & Caffrey, M. (2000). *Biomaterials*, **21**, 223–234.
Royant, A., Nollert, P., Edman, K., Neutze, R., Landau, E. M., Pebay-Peyroula, E. & Navarro, J. (2001). *Proc. Natl Acad. Sci. USA*, **98**, 10131–10136.
Rummel, G., Hardmeyer, A., Widmer, C., Chiu, M. L., Nollert, P., Locher, K. P., Pedruzzi, I. I., Landau, E. M. & Rosenbusch, J. P. (1998). *J. Struct. Biol.* **121**, 82–91.
Seddon, J. M., Templer, R. H., Warrender, N. A., Huang, Z., Cevc, G. & Marsh, D. (1997). *Biochim. Biophys. Acta*, **1327**, 131–147.
Templer, R. H. (1998). *Curr. Opin. Colloid Interface Sci.* **3**, 255–263.